



ELSEVIER

Journal of Immunological Methods xx (2006) xxx – xxx

**JIM**  
 Journal of  
 Immunological Methods

www.elsevier.com/locate/jim

Research paper

# The automated counting of spots for the ELISpot assay

 Natalie Hawkins <sup>\*</sup>, Steve Self, Jon Wakefield

*Fred Hutchinson Cancer Research Center, Statistical Center for HIV Aids Research and Prevention, 1100 Fairview Avenue, LE-400, Seattle, WA 98109, United States*

Received 15 March 2006; received in revised form 23 June 2006; accepted 10 August 2006

## Abstract

An automated method for counting spot-forming units in the ELISpot assay is described that uses a statistical model fit to training data that is based on counts from one or more experts. The method adapts to variable background intensities and provides considerable flexibility with respect to what image features can be used to model expert counts. Point estimates of spot counts are produced together with intervals that reflect the degree of uncertainty in the count. Finally, the approach is completely transparent and “open source” in contrast to methods embedded in current commercial software. An illustrative application to data from a study of the reactivity of T-cells from healthy human subjects to a pool of immunodominant peptides from CMV, EBV and flu is presented.

© 2006 Published by Elsevier B.V.

*Keywords:* Automated spot counting; ELISpot assay; Image analysis; Generalized linear models

## 1. Introduction

T-lymphocyte response to vaccination represents the primary immunogenicity endpoint in Phase I/II trials of current candidate HIV vaccines (Koup et al., 1994; Borrow et al., 1994; Rowland-Jones et al., 1995; Mazzoli et al., 1997; Musey et al., 1997; Ogg et al., 1998; Goh et al., 1999), and the use of a highly standardized, sensitive assay to measure these responses is a critical requirement in the development and evaluation of HIV vaccines. The ELISA-spot or ELISpot assay currently represents the primary

method to detect T-cell responses to HIV vaccines in the HIV Vaccine Trials Network. Considerable effort has been made to standardize the reagents and laboratory procedures used in these assays. However methods for the counting of spot-forming units (SFUs), which is used to obtain the final quantitative result of the ELISpot assay, have received somewhat less attention.

Historically, SFUs have been hand-counted by laboratory technicians but such subjective readings introduce significant variability in the assay outcome and are time-consuming. Computer algorithms for the analysis of images of the wells have been employed to automate the process of spot counting (Hudgens et al., 2004). Although automated spot counting algorithms can provide highly standardized assay outcomes, there are challenges to this approach that call into question the ultimate accuracy of these methods. Specifically, there is no “gold standard” for defining an SFU that can explicitly

*Abbreviations:* CMV, cytomegalovirus; EBV, Epstein–Barr virus; ELISpot, enzyme-linked immunospot; HIV, human immunodeficiency virus; T-cell, T-lymphocyte; SFU, spot-forming unit; TIFF, Tagged Image File Format.

<sup>\*</sup> Corresponding author. Tel.: +1 206 667 7753; fax: +1 206 667 4812.

*E-mail address:* [hawkins@scharp.org](mailto:hawkins@scharp.org) (N. Hawkins).

0022-1759/\$ - see front matter © 2006 Published by Elsevier B.V.

doi:10.1016/j.jim.2006.08.005

47 be used in algorithm design. In addition, such algorithms  
48 must integrate an automated method for calibration to  
49 background intensity levels that vary from plate to plate  
50 and distinguish “true SFUs” from various artifacts that  
51 include variable background intensity within wells (e.g.,  
52 edge effects) and contamination. Examples of images  
53 from ELISpot assays that illustrate some aspects of this  
54 variability are given in Fig. 1. Numbering from left to  
55 right and top to bottom, wells 1, 4 and 5 contain clear  
56 artifacts, while there are dark patches close to the edges of  
57 a number of wells.

58 In this work, we propose an automated approach to  
59 the analysis of images from ELISpot assays that

60 provides accurate and highly standardized counts of  
61 SFUs. In the absence of a gold standard for defining an  
62 SFU, we define the conceptual criterion of success for  
63 the method as a standardized implementation of the  
64 implicit rules for use by a designated expert (or possibly  
65 a panel of such experts) in counting SFUs. Specifically,  
66 the method uses “training data”, composed of SFU  
67 counts by an expert, in order to refine the algorithm to  
68 produce counts that are accurate reflections of the expert  
69 counts but, unlike counts by any human, are uniformly  
70 applied from assay to assay. The model-based approach  
71 we describe allows the uncertainty in the count to be  
72 acknowledged, so that an interval estimate for the

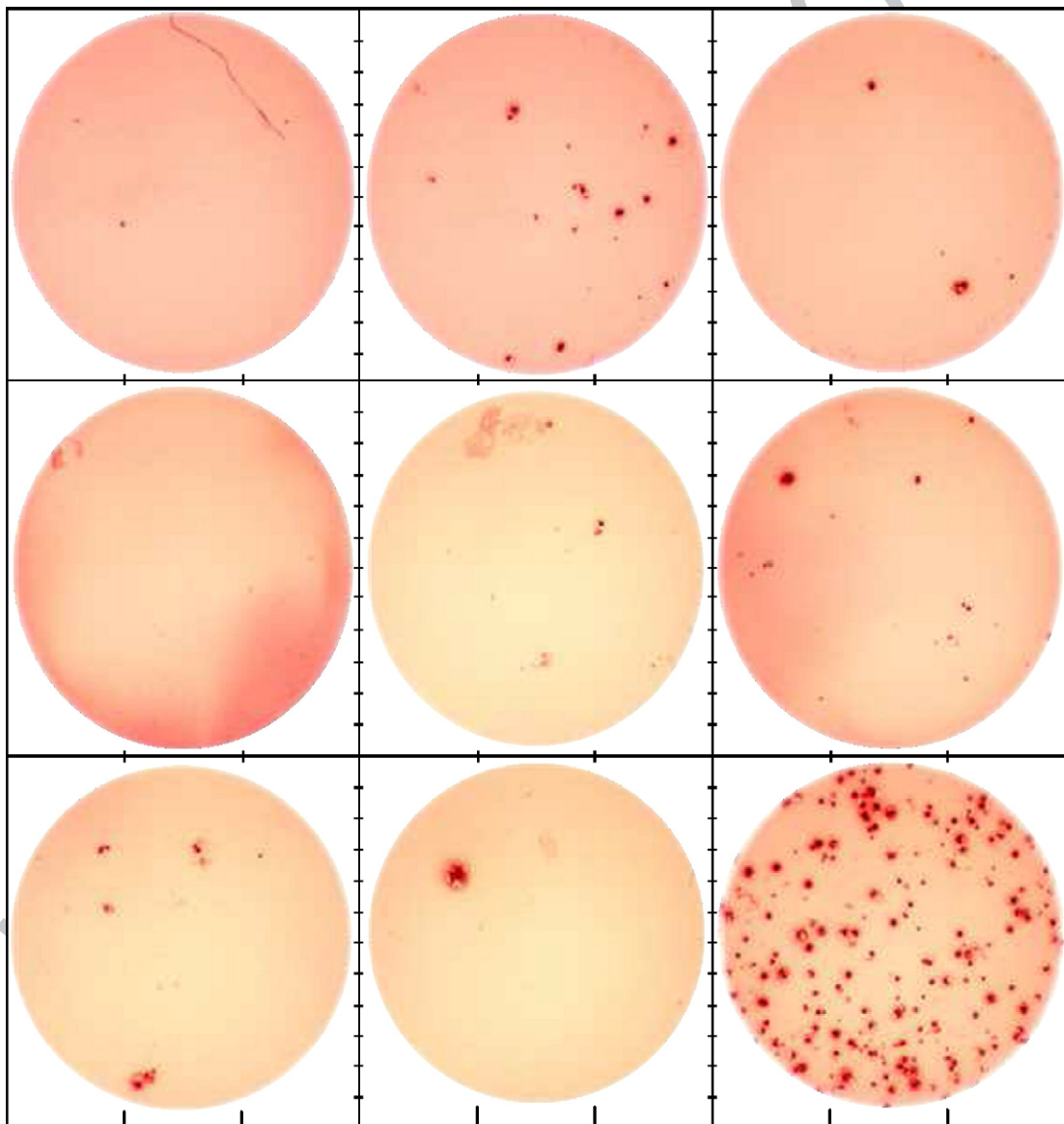


Fig. 1. Nine typical wells, showing spot forming units and various artifacts.

73 number of spots per well is produced. The method is  
 74 illustrated using data from a study of the reactivity of T-  
 75 cells from healthy human subjects to a pool of  
 76 immunodominant peptides from CMV, EBV and flu.

## 77 2. Methods

78 In this section we describe the method of assigning a  
 79 spot count to each well, along with an associated  
 80 interval estimate. The method has two components.  
 81 First, we pre-process the image using a thresholding and  
 82 grouping technique to identify interesting areas which  
 83 we call “globs”. Second, based on training data, we  
 84 formulate a model to predict the number of spots in each  
 85 glob, based on glob characteristics such as the size of the  
 86 glob. The resulting model is used to predict the number  
 87 of spots in a new well, along with an interval estimate.

### 88 2.1. Pre-processing

89 For each well, the raw data originate from a Tagged  
 90 Image File Format (TIFF) file and consist of pixel-level  
 91 red, green and blue intensities, displayed in Fig. 1. For  
 92 processing we use grey scale values by computing a  
 93 mean of the red, green, and blue values to get an intensi-  
 94 ty at each pixel. These values range from 0 to 255 and  
 95 are such that high intensities correspond to background,  
 96 while low intensities correspond to spots, and to  
 97 anomalies of the measurement process, such as an  
 98 errant hair in the well.

We use a thresholding technique, followed by a set of  
 grouping rules based on contiguity, to identify interest-  
 ing areas in the well which we call globs. We start with  
 globs rather than with SFUs, or spots, because the  
 thresholding technique easily identifies globs, but not  
 confluent spots within globs. A glob can contain zero or  
 one or more spots. We use a statistical model, described  
 later, to determine the number of spots within each glob.

We are first required to choose a thresholding value  
 to apply to a well to identify pixels belonging to globs.  
 Through empirical experimentation we chose, for each  
 well, the threshold to be the mean intensity of all pixels  
 in the well minus three standard deviations, the latter  
 calculated over all pixels in the well. Fig. 2 illustrates,  
 with the histogram of intensities for the ninth well in  
 Fig. 1 and the associated threshold.

Globs are identified in the well by first comparing  
 each well pixel to the threshold. If the pixel intensity is  
 below the threshold, the pixel is called a glob pixel, and  
 globs are formed from glob pixels based on contiguity  
 of those pixels. For one pixel globs, none of the possible  
 eight pixels surrounding the one glob pixel is a glob  
 pixel. For multiple-pixel globs, each pixel in the glob  
 must be touching another glob pixel in, at least, one of  
 the possible eight positions surrounding the pixel. Once  
 the globs have been identified, we drop small, light  
 globs since, in discussion with the lab technicians, these  
 do not correspond to real spots. “Small” means less than  
 10 pixels and “light” corresponds to average intensity  
 greater than 95% of the threshold value used to make the  
 glob/not-glob pixel assignment (recall that high intensi-  
 ty values mean that the spot is light, not dark). As an  
 example, the left-hand panel of Fig. 3 reproduces the  
 ninth well in Fig. 1, with the right-hand panel showing  
 the globs that have been identified using the threshold-  
 ing technique.

Next we formulate a statistical model, based on  
 training data, which can be used to predict the number of  
 spots within each glob and, as a result, the number of  
 spots in a new well, along with a confidence interval.

### 2.2. Training data

We use a set of training data to build a predictive  
 statistical model, based on glob characteristics, which  
 can be used to predict the number of SFUs, or spots, in a  
 well, along with an interval estimate. The statistical  
 model requires, as input, data from globs identified in  
 the well.

The training data consist of glob data from 50 wells,  
 selected from three plates. For each glob we obtained an  
 “expert” count of the number spots within the glob. The

**Histogram of Pixel Intensities in a Well**

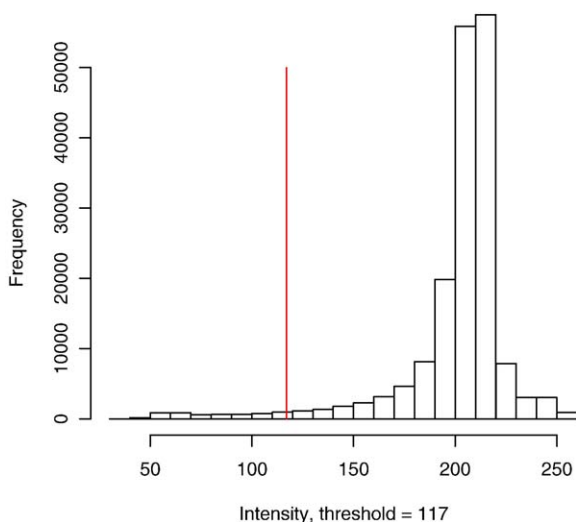


Fig. 2. Histogram of intensities from the ninth well in Fig. 1. The vertical line corresponds to the “threshold”.

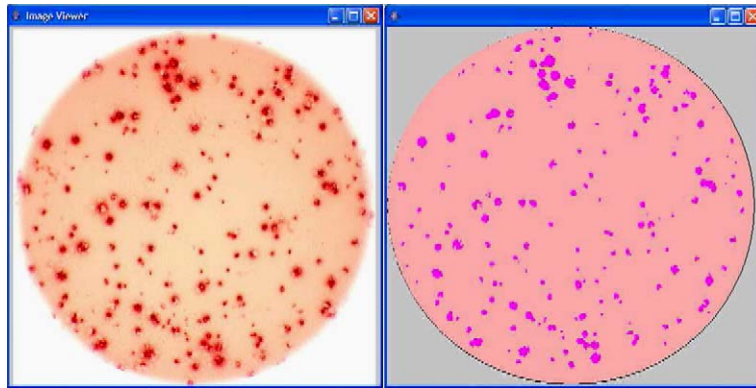


Fig. 3. The image on the right shows the globs identified in the well on the left using the thresholding technique. This well is the ninth well in Fig. 1.

149 “expert” count of the number of spots within each glob  
 150 was provided by a senior immunologist. We provided  
 151 the expert with an Excel spreadsheet which contained  
 152 one page per well. On each page we displayed the  
 153 original TIFF image of the well, along with numbered,  
 154 computer-generated arrows super-imposed on the image  
 155 pointing to globs, which we had identified using the  
 156 thresholding and grouping technique described above.  
 157 In areas of high congestion, outlines were drawn to  
 158 separate globs. To the right of the image, a data entry  
 159 area was provided with a column displaying the glob  
 160 numbers and an empty column for the number of spots  
 161 judged to be within each glob. The expert examined  
 162 each image, and entered the number of spots for each  
 163 glob.

164 Discussions with the expert revealed a set of rules  
 165 that were used when counting spots. True spots are dark  
 166 in the center and slightly fuzzy on the edges. False spots  
 167 are either: (1) very faint and/or very small, (2) clustered  
 168 at the edges of the well, (3) aligned in a hair-like pattern  
 169 (indicates a cracked well), or (4) look like debris (very  
 170 dark and often not circular). The characteristics of the  
 171 globs that we chose to investigate were based on these  
 172 rules, and on our empirical observations of what glob  
 173 characteristics were important predictors of the number  
 174 of spots in each glob.

175 The nine glob characteristics were: (1) glob size, (2)  
 176 median intensity within glob, (3) ratio of maximum glob  
 177 intensity to minimum glob intensity, (4) variance of glob  
 178 intensity, (5) ratio of variance of glob intensity to mean  
 179 glob intensity, (6) median distance of the glob from the  
 180 center of the well, (7) whether or not the glob is located  
 181 near the edge of the well, which is defined as whether or  
 182 not the median distance of the glob from the center of  
 183 the well is greater than 75% of the longest radius in the  
 184 well (the well is almost, but not quite a perfect circle),  
 185 (8) the percent of the pixels in the box which bounds the

glob which are glob pixels, (9) the square of the log of  
 the ratio of the dimensions (height and width) of the box  
 which bounds the glob.

### 2.3. Statistical modeling

Based on training data, we aim to form a model,  
 which entails selecting glob characteristics on the basis  
 of their ability to predict the number of spots in each  
 glob. We build all possible models having from just one  
 to all nine of the glob characteristics as covariates  
 ( $2^9 - 1 = 511$  models), as well as all possible combina-  
 tions involving interaction terms with the discrete glob  
 characteristic edge (an additional 6305 models). A  
 cross-validating procedure, described later, is used to  
 select the best model from the complete set of 6816  
 possible models. The best model can then be used to  
 predict the number of spots in any future wells, based on  
 the glob characteristics of those wells.

We select a set of  $n$  training wells, pre-processed as  
 described in Section 2.1, containing a set of globs with  
 glob characteristics  $X_{ij}$  for glob  $j$  within training well  $i$ ;  
 accompanying each well and glob is a number of spots,  
 $Y_{ij}$ ,  $i = 1, \dots, n$ ,  $j = 1, \dots, g_i$ , as counted by the lab  
 technician.

Since the outcome is discrete, a natural starting point  
 for analysis is a Poisson model with mean number of  
 counts  $E[Y_{ij}|X_{ij}]$ . Unfortunately such a model is  
 deficient in the sense that the Poisson assumption  
 constrains the variance to equal the mean. As described  
 in McCullagh and Nelder (1989), a more flexible  
 working model assumes that  $\text{var}(Y_{ij}|X_{ij}) = \kappa \times E[Y_{ij}|X_{ij}]$ ,  
 so that  $\kappa$  allows the variance to deviate from that under  
 a Poisson model. We also assume that the mean takes  
 the log-linear form

$$\log E[Y_{ij}|X_{ij}] = X_{ij}\beta,$$



t1.1 Table 1  
t1.2 Summary of parameter estimates from best-fitting model

t1.3 Characteristic	Estimate	Standard error	p-value
t1.4 Located near edge	1.20	0.859	0.164
t1.5 Height–width ratio	−0.0901	0.3186	0.7775
t1.6 Median intensity in glob	−0.0325	0.00362	$2.0 \times 10^{-16}$
t1.7 Variance of intensities in glob	0.00447	0.000427	$2.0 \times 10^{-16}$
t1.8 Ratio of variance to mean intensities in glob	−0.606	0.0608	$2.0 \times 10^{-16}$
t1.9 Glob size	0.000105	0.000313	0.737
t1.10 Median distance of glob from the center of the well	−0.000308	0.000955	0.747
t1.11 Ratio of max to min intensity in glob	0.279	0.0867	0.00135
t1.12 Edge×height–width ratio	−1.74	0.634	0.00620
t1.13 Edge×size	0.000418	0.000532	0.433
t1.14 Edge×median distance from center of well	−0.00560	0.00420	0.183

219 though our method could use any form. For example,  
221 the method we describe could be applied to any  
222 parametric or semi-parametric model including logic  
223 regression, generalized additive models, or splines, see  
224 [Hastie, Tibshirani, and Friedman \(2000\)](#) for more detail  
225 on these methods. A quasi-likelihood method of  
226 inference, as described in [McCullagh and Nelder \(1989\)](#),  
227 is used to estimate the parameters of the model; this  
228 method has the advantage of requiring the specification  
229 of the first two moments of the data, without making a  
230 distributional assumption. The method we describe can  
231 also be used with specific distributional assumptions, if  
232 these appear reasonable in any particular application.  
233 We also use sandwich estimation ([Royall, 1986](#)) to provide  
234 empirical estimates of the standard errors. This approach  
235 provides a consistent estimator of the standard errors,  
236 given independent glob counts.

238 The over-dispersion parameter, along with sandwich  
239 estimation, is designed to account for components of  
240 variation that are attributed to well and/or plate.  
241 Although there are methods for improving prediction  
242 error of counts for one well using data from other wells  
243 on the same plate, in our experience working with  
244 laboratory scientists, they prefer to make prediction  
245 for each well independently. We wish to have a general  
246 method and not one which needs retuning in each  
247 different scenario.

248 Once we have selected the best predictive model of  
249 the type described above, based on the training data,  
250 the model can be used to predict the number of spots  
251 in a new well. Let  $X_j$  denote the glob characteristics  
252 of a new well containing  $j=1, \dots, n_{\text{new}}$  globs, for  
253 which we require an estimate of the number of spots,  
call this  $\hat{\theta}$ .

254 Once estimates  $\hat{\beta}$  and  $\hat{\kappa}$  are obtained, a prediction is  
255 available via  $\hat{\theta} = \sum_{j=1}^{n_{\text{new}}} \exp(X_j \hat{\beta})$ , which is an unbiased  
256 estimate.

257 Using the delta method to obtain the variance of  $\hat{\theta}$ ,  
258 we obtain an approximate 95% interval for the total  
259 number of spots that is given by:

$$\sum_{j=1}^{n_{\text{new}}} \exp(X_j \hat{\beta}) \pm 1.96 \times \left[ \left\{ \sum_{j=1}^{n_{\text{new}}} \exp(X_j \hat{\beta}) X_j \right\} \hat{V} \left\{ \sum_{j=1}^{n_{\text{new}}} X_j^T \exp(X_j \hat{\beta}) \right\} \right]^{1/2}$$

where  $\hat{V}$  is the sandwich estimate of the variance of  $\hat{\beta}$ . 260

### 3. Results 262

263 We wish to use the training data to decide on which  
264 of the 9 glob characteristics are important predictors of  
265 the number of spots that each glob contains, in order to  
266 find the model which would best serve as a predictive  
267 model. Specifically we have a total of  $K=6816$  models,  
268 this set consisting of all possible models containing or  
269 not-containing each of the 9 glob characteristics, as well  
270 as all possible interaction models containing an  
271 interaction with the discrete glob characteristic, edge.  
272 We use a cross-validation technique, in which we use 49  
273 of the training wells to estimate the parameters of model,  
274  $M_k, k=1, \dots, K$ , and then predict the number of spots in

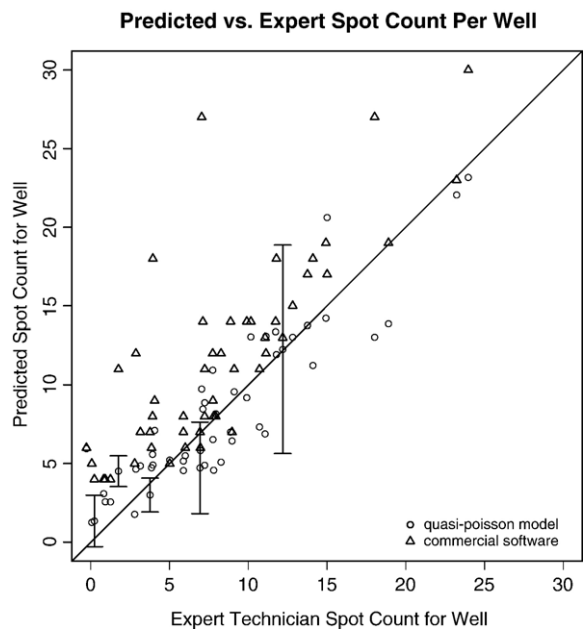


Fig. 4. Number of spots as predicted by the model-based approach and the current automated lab method, for 50 wells.

275 the 50th well; repeating this procedure and leaving out a  
 276 different well each time, gives a set of predictions  $\hat{Y}_{ij}^k$   
 277 under model  $k$ , so that we can calculate the model  
 278 assessment sum of squares criteria

$$SS_k = \sum_{i=1}^n \sum_{j=1}^{g_i} (Y_{ij} - \hat{Y}_{ij}^k)^2,$$

280  $k=1, \dots, K$ . After training the model with data from  
 281 globs from 50 wells, we found the best model, based on  
 282 the minimum  $SS_k$ .

283 The best model was found to contain eight glob  
 284 characteristics and three interaction terms with the glob  
 285 characteristic edge: (1) edge, (2) height–width ratio,  
 286 defined as the square of the log of the ratio of the  
 287 dimensions (height and width) of the box which bounds  
 288 the glob, (3) median intensity, (4) variance of the  
 289 intensity, (5) variance of the intensity divided by the  
 290 mean intensity, (6) size, (7) median distance from the  
 291 center of the well, (8) the ratio of the maximum intensity  
 292 to the minimum intensity; and interactions of edge with:  
 293 (1) height–width ratio, (2) size, and (3) median distance  
 294 from the center of the well. Once we have decided upon  
 295 this model we re-estimate the coefficients based on all  
 296 50 wells. Table 1 contains the resulting estimates, along  
 297 with their standard errors.

298 From the coefficients we see that globs classified as  
 299 near the edge are more likely to contain more spots. The  
 300 more rectangular the glob is, as measured by the height–  
 301 width ratio, the less likely it is to contain more spots.  
 302 Darker globs (as measured by lower median intensity)  
 303 are more likely to contain more spots, while more  
 304 constant intensity within a glob implies fewer spots. As  
 305 the ratio of the variance of the intensity to the mean  
 306 intensity increases the number of spots decreases. Globs  
 307 containing more pixels are more likely to contain more  
 308 spots. Globs that are located further from the center of  
 309 the well are more likely to contain fewer spots  
 310 (reflecting the anomalies that occur towards the outside  
 311 of the well, see Fig. 1, wells 4 and 6 in particular).  
 312 Finally, greater maximum to minimum intensities  
 313 suggest more spots also. Looking at the interaction  
 314 terms we see that globs near the edge and more  
 315 rectangular (as measured by the height–width ratio) are  
 316 likely to contain fewer spots. Larger globs near the edge  
 317 are more likely to contain more spots, and globs  
 318 classified as near the edge but which are closer to the  
 319 edge are likely to contain fewer spots. The non-  
 320 significance of four of the variables and two of the  
 321 interaction terms, is perhaps surprising but it is the  
 322 combination of variables that is important from a  
 323 prediction point of view.

Fig. 4 shows the estimated number of spots in each of  
 the 50 wells from our method, versus those from the  
 laboratory expert. Also shown are the estimates from the  
 automated method currently used by the lab. For clarity,  
 for a small collection of wells we include our confidence  
 interval, based on the sandwich estimator of the  
 variance. For plotting, we have jittered the values on  
 the  $x$ -axis slightly to uncover points which might be  
 overlapping so that all 100 points are visible on the plot.  
 We see that the model predictions are more accurate  
 relative to the expert technician, than is the commercial  
 software being used by the lab. As confirmation of  
 this we can evaluate the average bias, given by  
 $1/n \sum_{i=1}^n (Y_i - \hat{Y}_i)$ , and the mean squared error (MSE),  
 given by  $1/n \sum_{i=1}^n (Y_i - \hat{Y}_i)^2$ , where  $Y_i$  and  $\hat{Y}_i$  are the  
 observed and predicted number of spots in well  $i$ , for  
 each of the model-based and current automated lab  
 methods. For the model-based approach we obtain an  
 average bias and MSE of 0.0336 and 5.68, while for  
 the current automated lab method we obtained average  
 bias and MSE of 3.49 and 26.4. Hence we see the  
 model-based approach provides more accurate pre-  
 dicted numbers of spots, as measured by both bias and  
 precision; in particular the commercial software  
 provides an overcount of the number of spots.

#### 4. Discussion

There is no “gold standard” method of spot counting  
 to which automated methods can be compared. In the  
 absence of such a standard, expert opinion with all of its  
 associated vagaries, represents the standard by which  
 automated methods must be judged. However expert  
 opinion must first be operationally defined. We have  
 operationally defined expert opinion in this work as the  
 counts made on our training data set by a senior  
 immunologist with whom we have collaborated. This  
 has served our purpose of providing a realistic and  
 pertinent illustration of a specific application of our  
 proposed method. A broader definition based on a panel  
 of immunologists might also have been used. We leave  
 to future work the development of a more extensive set  
 of training data together with an associated consensus  
 expert opinion of spot counts that might provide a more  
 definitive and broadly applicable counting algorithm  
 based on our methods.

The accuracy of an automated counting method refers  
 to how faithfully the method replicates the counts from  
 expert opinion on average (over globs). Our proposed  
 method is trained directly from expert opinion using  
 statistical methods that guarantee (in large samples) such  
 accuracy. We expect that this will provide a more

374 accurate reproduction of counts based on expert opinion  
375 than other methods that are indirectly “calibrated”.

376 Assessing the precision of automated methods is  
377 challenging because there is innate non-systematic  
378 variability in expert opinion. This variability is reflected  
379 in the fact that expert recounts do not always result in  
380 exactly the same number of spots per well. This  
381 component of random variation will be inherited by  
382 any automated method. The proposed counting method  
383 is based on measurable characteristics of globs and, to  
384 the extent that these characteristics capture all factors  
385 considered systematically by experts in their counts, the  
386 automated methods will faithfully replicate the expert  
387 opinion up to the aforementioned random variability.  
388 We expect that a certain amount of systematic variation  
389 in expert counts will not be captured by readily  
390 measurable glob characteristics so that automated  
391 methods will inevitably be somewhat more variable  
392 than the theoretical minimum variation defined by  
393 recount variability. However, the proposed method is  
394 completely flexible with respect to the set of measurable  
395 glob characteristics that can be considered as possible  
396 predictors with practical limits on this set imposed only  
397 by the size of the training data set. Thus, with an  
398 extensive training data set and careful elicitation of the  
399 glob characteristics and other factors considered by  
400 experts in performing their counts, it is reasonable to  
401 expect that the proposed method will reproduce the  
402 systematic variation in expert counts.

403 One advantage of the proposed method is that  
404 interval estimates of spot counts are naturally produced  
405 that reflect the degree of uncertainty in the count. This  
406 interval estimate can be used as a component of the  
407 assay quality control process to reflect reliability of  
408 counts delivered for each well. The estimated variability  
409 in spot count at the well level can also form the basis for  
410 a similar estimate of variability for summary measures  
411 of response that combine spot counts over multiple  
412 wells (e.g. total response across peptide-treated wells net  
413 of response in negative control wells).

414 Finally, the proposed method provides a completely  
415 transparent “open-source” approach for spot counting  
416 that is in contrast to proprietary methods embedded in  
417 commercial software that often function as a black-box.  
418 In the current atmosphere that places considerable value  
419

419 on standardization of reagents and operating procedures  
420 for immunologic assays used in the development and  
421 evaluation of HIV vaccines (Klausner et al., 2003), the  
422 proposed method represents a natural approach to  
423 extending this standardization to the final critical step  
424 of the assay process.

## References

- 425
- Borrow, P., Lewicki, H., Hahn, B.H., Shaw, G.M., Oldstone, M.B., 426  
1994. Virus-specific CD8-cytotoxic T-lymphocyte activity associ- 427  
ated with control of viremia in primary human immunodeficiency 428  
virus type 1 infection. *Journal of Virology* 68, 6103. 429
- Goh, W.C., Markee, J., Akridge, R.E., et al., 1999. Protection against 430  
human immunodeficiency virus type 1 infection in persons with 431  
repeated exposure: evidence for T cell immunity in the absence of 432  
inherited CCR5 coreceptor defects. *Journal of Infectious Diseases* 433  
179, 548. 434
- Hastie, T., Tibshirani, R., Friedman, J., 2000. *The Elements of* 435  
*Statistical Learning, Data Mining, Inference and Prediction.* 436  
Springer, Verlag. 437
- Hudgens, M., Self, S., Chiu, Ya-Lin, et al., 2004. Statistical 438  
considerations for the design and analysis of the ELISpot assay 439  
in HIV-1 vaccine trials. *Journal of Immunological Methods* 288, 440  
19. 441
- Klausner, R.D., Fauci, A.S., Corey, L., 2003. The need for a global 442  
HIV vaccine enterprise. *Science* 300, 2036. 443
- Koup, R.A., Safrit, J.T., Cao, Y., Andrews, C.A., McLeod, G., 444  
Borkowsky, W., Farthing, C., Ho, D.D., 1994. Temporal association 445  
of cellular immune responses with the initial control of viremia in 446  
primary human immunodeficiency virus type 1 syndrome. *Journal of* 447  
*Virology* 68, 4650. 448
- Mazzoli, S., Trabattoni, D., Lo Caputo, S., et al., 1997. HIV-specific 449  
mucosal and cellular immunity in HIV-seronegative partners of 450  
HIV-seropositive individuals. *Nature Medicine* 3, 1250. 451
- McCullagh, P., Nelder, J.A., 1989. *Generalized Linear Models*, Second 452  
edition. Chapman and Hall. 453
- Musey, L., Hughes, J., Schacker, T., Shea, T., Corey, L., McElrath, M.J., 454  
1997. Cytotoxic-T-cell responses, viral load, and disease progression 455  
in early human immunodeficiency virus type 1 infection. *New* 456  
*England Journal of Medicine* 337, 1267. 457
- Ogg, G.S., Jin, X., Bonhoeffer, S., Dunbar, P.R., Nowak, M.A., 458  
Monard, S., Segal, J.P., Cao, Y., Rowland-Jones, S.L., Cerundolo, 459  
V., Hurley, A., Markowitz, M., Ho, D.D., Nixon, D.F., McMichael, 460  
A.J., 1998. Quantitation of HIV-1-specific cytotoxic T lympho- 461  
cytes and plasma load of viral RNA. *Science* 279, 2103. 462
- Rowland-Jones, S., Suttone, J., Ariyoshi, K., et al., 1995. HIV-specific 463  
cytotoxic T-cells in HIV-exposed but uninfected Gambian women. 464  
*Nature Medicine* 1, 59. 465
- Royall, R., 1986. Model robust confidence intervals using maximum 466  
likelihood estimators. *International Statistical Review* 54, 221. 467  
468